Elimination of Gibbs' Phenomena from Error Analysis of Finite Element Results

Gaylen A. Thurston*
NASA Langley Research Center, Hampton, Virginia 23665
and
Rajaram Sistla†
Analytical Services & Materials, Inc., Hampton, Virginia 23665

A change of variables is presented that improves the accuracy of Fourier half-range sine series used in numerical harmonic analysis. The change in variables, a simple but effective extension of the period of the series, results in an interpolation formula that passes through the endpoints of tabulated data. In two dimensions, the change in variables produces an "extended grid" for use in computing coefficients in double sine series. The improved double sine series was developed for modifying a postprocessor code for error analysis of results from a general-purpose finite element code. Without going into the details of the error analysis, the paper illustrates the improved numerical harmonic analysis by applying it to the problem of a simply supported plate under uniform load. The elimination of Gibbs' phenomenon from the truncated series for the uniform load and from a discrete set of boundary conditions suggests that the extended grid transformation can be applied readily in a postprocessor for error analysis of discrete results for postbuckled stiffened panels.

Nomenclature

A_{mn}, w_{mn}	= Fourier coefficients in double sine series
a,b	= length and width of rectangular plate
D	= plate bending stiffness
$E_N(x,y)$, $E_I(x,y)$	= normalized residual errors
K	= factor in Fourier coefficient
K_w, K_M, K_Q	= nondimensional factors in results for w, M_x, and Q_x
M_x	= moment stress resultant
Q_x	= transverse shear stress resultant
q	= constant uniform transverse load
w	= solution of plate equation
w_E	= solution of biharmonic equation
w_I	= particular solution of plate equation as double Fourier series in extended grid coordinates
w_N	= Navier solution of simply supported plate problem
w_r	= solution based on displacement/rotation boundary conditions
x,y	= Cartesian coordinates on plate
α,δ	= constant factors in coordinate transformation
α_n, δ_m	= coefficients in exponential solutions in w_E
δ_{ij}	= Kronecker delta
ξ,η	= transformed coordinates on extended grid

Presented as Paper 90-0932 at the AIAA/ASME/ASCE/AHS/ASC 31st Structures, Structural Dynamics, and Materials Conference, Long Beach, CA, April 2-4, 1990; received May 22, 1990; revision received Nov. 2, 1990; accepted for publication Nov. 13, 1990.

*Senior Aerospace Engineer, Structural Mechanics Branch, Structural Mechanics Division, MS-190. Associate Fellow AIAA.
†Research Engineer. Senior Member AIAA.

Introduction

ESTIMATING the accuracy of stresses and deflections computed by the finite element method is a common problem that arises with each application of the method. A general approach to error analysis is outlined in Ref. 1. The approach uses Newton's method applied to the Euler equations of shell theory. In earlier papers, small finite-deflection theory was used. Numerical results are reported in Refs. 1-3 for buckled rectangular skin sections from flat panels and from cylindrical panels. Other approaches to error analysis have been proposed by Zienkiewicz and Zhu[4,6] Ainsworth et al.,[5] and Dow et al.[7,8]

The present paper is concerned with a small, but basic, problem that arose in the previous studies of error analysis. The problem is to compute continuous approximations from discrete finite element results. The continuous approximation in the earlier papers exhibited an error similar to Gibbs' phenomenon for Fourier series; the error was much higher near the boundary of rectangular skin sections than at points away from the boundary.

The continuous approximation is integrated by successive approximations to obtain an approximate continuous solution of the shell problem. The continuous solution yields numerical results for stress resultants and deflections that can be compared with corresponding results from the finite element solution. However, the existence of Gibbs' phenomena in the approximations introduces an unknown factor in assessing the error in the finite element results for nonlinear shell problems.

Therefore, the main topic of this paper is the numerical harmonic analysis of double Fourier sine series used to approximate continuous functions. The functions are computed from discrete data tabulated on a rectangular grid. The approximation is improved by a simple change of variables. The change of variables can be visualized by extending the rectangular grid by two rows and by two columns. The approximation computed by this change of variables will be called the "extended grid approximation."

A second topic of the paper, which is a consequence of using the extended grid, is the problem of satisfying discrete boundary conditions. The extended grid approximation is applied to the uniform load term in the linear plate bending equation. The approximation is integrated to obtain a continuous solution. The solution based on the extended grid does

not satisfy the boundary conditions for the example of the simply supported plate. A solution of the biharmonic equation is derived and superposed to satisfy the boundary conditions at discrete points on the plate boundary. The number of discrete points on the boundary used in the solution is the same as those on the edges of the rectangular grid, since in the application of the approximations to finite element results, numerical results on the boundary are known only at nodal points of the finite element grid.

Extended Grid Solution for a Simply Supported Plate Under Constant Uniform Load

A familiar example of Gibbs' phenomenon is in the Navier solution[9] for a simply supported plate under a uniform load q. The linear problem is the bending of an isotropic plate of length a and width b. The Navier solution for the transverse deflection w is written in the form of a double Fourier sine series,

$$w = \sum_{m=1}^{M} \sum_{n=1}^{N} w_{mn} \sin \frac{m\pi x}{a} \sin \frac{n\pi y}{b} \tag{1}$$

The Fourier coefficients w_{mn} are derived by substituting the series for w in the equation for plate bending,

$$\nabla^4 w = q/D \tag{2}$$

The constant q/D is approximated by a double Fourier sine series so that w actually satisfies the following equation:

$$\nabla^4 w_N = \left[\frac{16q}{\pi^2 D}\right] \sum_{m=1,3}^{M} \sum_{n=1,3}^{N} \frac{1}{mn} \sin \frac{m\pi x}{a} \sin \frac{n\pi y}{b} \tag{3a}$$

$$w_N = \left[\frac{16q}{\pi^2 D}\right] \sum_{m=1,3}^{M} \sum_{n=1,3}^{N} \frac{1}{mn} \frac{\sin(m\pi x/a) \sin(n\pi y/b)}{\pi^4[(m/a)^2 + (n/b)^2]^2} \tag{3b}$$

On the plate boundaries, $x = 0$, $x = a$, $y = 0$, and $y = b$, $\nabla^4 w_N$ in Eq. (3a) is zero, and obviously, w_N does not satisfy the differential equation for w [Eq. (2)]. As the upper limits of the series, M and N, approach infinity and for every fixed point (x,y) inside the boundary, the series expression converges to q/D. However, at a point with the approximate coordinates $x = a/(M + 1)$ and $y = b/(N + 1)$, the sum of the series defined in Eq. (3a) is approximately 1.4 (q/D). In other words, the normalized residual error for the Navier solution,

$$E_N(x,y) = (D/q)\nabla^4 w_N - 1 \tag{4}$$

attains a relative maximum value of 40% and is -1 on the plate boundary. This property of Fourier sine series of overshooting in approximating discontinuities in periodic functions is known as Gibbs' phenomenon (see, for example, Refs. 10 and 11).

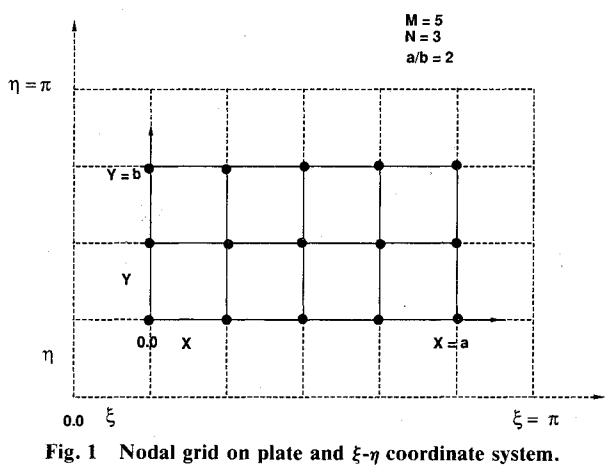

Fig. 1 Nodal grid on plate and ξ-η coordinate system.

The Gibbs' phenomenon for the example problem is associated with the jump in $\nabla^4 w$ from zero on the boundary to the nonzero value q/D. To avoid Gibbs' phenomenon, the analysis is altered by using an extended grid and numerical harmonic analysis. The extended grid is illustrated for a single Fourier sine series to approximate a function $f(x)$ of one independent variable in Appendix A. The numerical harmonic analysis to approximate a function $f(x,y)$ of two variables by a double Fourier sine series on the extended grid shown in Fig. 1 is given in Appendix B.

The new series for $\nabla^4 w$ is written in the form

$$\nabla^4 w = \sum_{m=1}^{M} \sum_{n=1}^{N} A_{mn} \sin m\xi \sin n\eta \tag{5}$$

where the change of independent variables is

$$\xi = \frac{\pi}{M+1}[(x/a)(M-1) + 1], \qquad 0 \le \xi \le \pi \tag{6a}$$

$$\eta = \frac{\pi}{N+1}[(y/b)(N-1) + 1], \qquad 0 \le \eta \le \pi \tag{6b}$$

The change of independent variables is shown graphically in Fig. 1 for a plate with aspect ratio $a/b = 2$ and a grid with $M = 5$ nodes in the x direction and $N = 3$ nodes in the y direction. The origin of the nondimensional ξ-η coordinate system is outside the plate, as indicated by the dotted lines showing the coordinate axes. The $M \times N$ array of Fourier coefficients A_{mn} in Eq. (5) is computed by numerical harmonic analysis so that $\nabla^4 w$ passes through the value of q/D at every nodal point on the plate, including all nodal points on the plate boundary.

The numerical harmonic analysis for expanding the constant q/D in the double sine series on the extended grid is a special case of expanding a function $f(x,y)$, as described in Appendix B. The coefficients A_{mn}, in the approximation for q/D in Eq. (5), are computed by applying the formula in Eq. (B4),

$$A_{mn} = \frac{2}{M+1} \frac{2}{N+1} \sum_{j=1}^{M} \sum_{k=1}^{N} \frac{q}{D} \sin m\xi_j \sin n\eta_k \tag{7}$$

A solution of Eq. (5), denoted as w_I, is

$$w_I = \sum_{m=1}^{M} \sum_{n=1}^{N} \frac{A_{mn}}{[(m\delta)^2 + (n\alpha)^2]^2} \sin m\xi \sin n\eta \tag{8}$$

where

$$\delta = \frac{\pi(M-1)}{a(M+1)}, \qquad \alpha = \frac{\pi(N-1)}{b(N+1)}$$

The normalized error for this solution is defined as

$$E_I(x,y) = (D/q)\nabla^4 w_I - 1 \tag{9}$$

For the same finite values of M and N, the limits on the sum of each series, the new series w_I is a more accurate solution of the plate equation than the Navier solution w_N.

The increased accuracy in approximating q/D is illustrated in Figs. 2 and 3. The contour plot of $E_I(x,y)$ in Fig. 2 has a maximum error near the corners of 10.8% for an $M = 9$ by $N = 9$ grid and zero error on the boundary. The comparable value for the error $E_N(x,y)$ is 40% near the corners and -1 on the boundary. The two normalized errors are compared directly along a line of symmetry, $y = b/2$, of the plate in Fig. 3. The zeros of $E_I(x,y)$ occur at node points of the grid.

However, w_I, the solution for w derived from the new series for q/D in Eq. (5), does not satisfy the simply supported boundary conditions. An additional solution of the biharmonic equation is added to the solution w_I to satisfy the

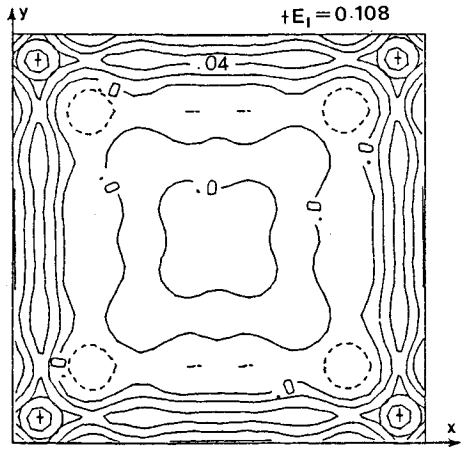

Fig. 2 Normalized error in transverse equilibrium equation $E_I(x,y)$.

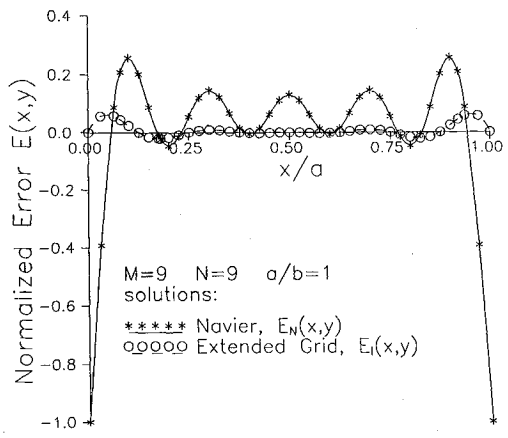

Fig. 3 Normalized error $E(x,y)$ along the line $y/b = 0.5$.

boundary conditions. The additional solution w_E is assumed in the form

$$w_E = \sum_{n=1}^{N} f_n(x) \sinh n\eta + \sum_{m=1}^{M} g_m(y) \sin m\xi \tag{10}$$

and is selected with the idea of applying the solution to error analysis of finite element solutions for plates. In the finite element error analysis, the boundary conditions are known only at node points. Therefore, the upper limits M and N for the two series in Eq. (10) correspond to the number of nodes used to generate the solution w_I. Since the sine terms in w_E do not vanish on the boundary, nonhomogeneous boundary conditions can be satisfied by the functions in Eq. (10). Earlier studies[1-3] included series of cosine terms in a similar solution, making a total of four series. Using only two series in w_E simplifies the algebra in satisfying the boundary conditions.

The solution w_E satisfies the biharmonic equation

$$\nabla^4 w_E = 0 \tag{11}$$

term by term. The expressions for the functions $f_n(x)$ and $g_m(y)$ are listed in Appendix C.

Each of the solutions $f_n(x)$ and $g_m(y)$ contains four constants of integration for a total of $4(M + N)$. The numerical results in the next section are computed using two different sets of constants of integration. The two sets of constants are computed from two different sets of discrete boundary conditions. The condition of $w = 0$ at node points on the boundary is in both sets of discrete boundary conditions. In addition, one set of discrete conditions at node points contains the natural boundary condition for the simply supported plate that the moment stress resultant must vanish.

The second set of conditions uses a discrete set of geometric conditions on the derivative of w in the direction of the outward normal. These slopes are output data from a general-purpose finite element code. This choice of boundary conditions is part of the general approach to error analysis outlined in Ref. 1.

In either case, the normalized error for the solution

$$w = w_I + w_E \tag{12}$$

does not depend on the boundary conditions. By definition,

$$E_w(x,y) = (D/q)\nabla^4(w_E + w_I) - 1$$
$$= E_I(x,y) \tag{13}$$

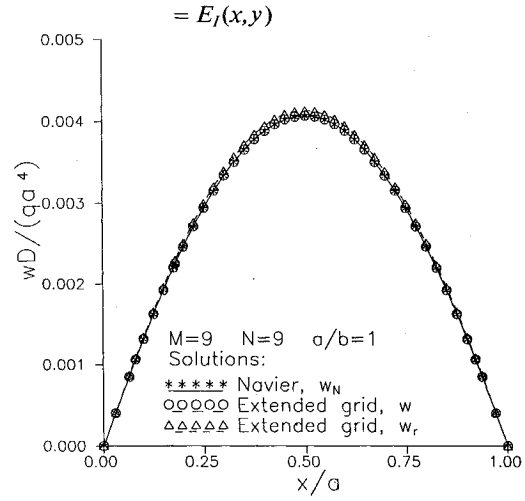

Fig. 4a Transverse deflection w along the line $y/b = 0.5$.

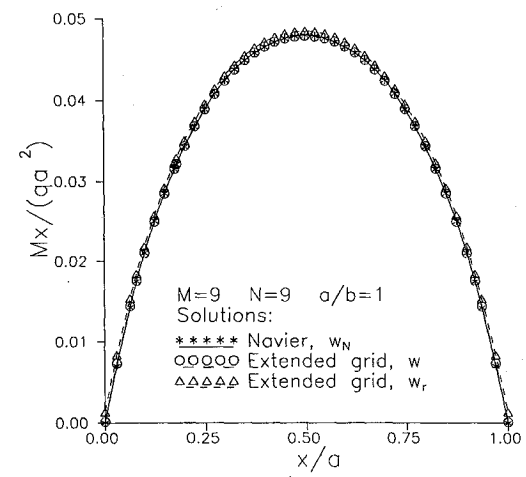

Fig. 4b Moment resultant M_x along the line $y/b = 0.5$.

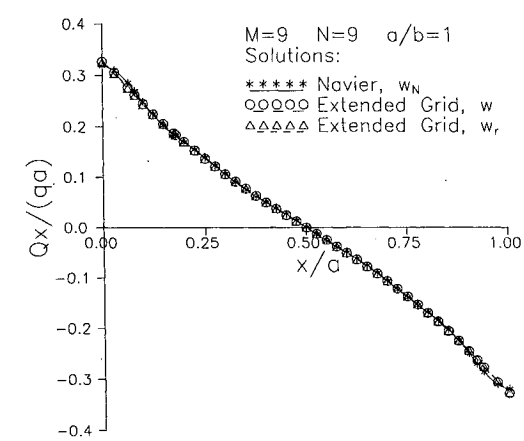

Fig. 4c Transverse shear stress resultant Q_x along the line $y/b = 0.5$.

Table 1 Comparison of extended grid solution to exact Navier solution for simply supported plate

	K_w in $W_{max} = K_w qa^4/D$			K_M in $M_{x_{max}} = K_M qa^2$			K_Q in $Q_{x_{max}} = K_Q qa$		
	Extended grid solution		Navier	Extended grid solution		Navier	Extended grid solution		Navier
b/a	$M = 5 \times N = 5$	$M = 9 \times N = 9$	solution	$M = 5 \times N = 5$	$M = 9 \times N = 9$	solution	$M = 5 \times N = 5$	$M = 9 \times N = 9$	solution
1.0	0.00407	0.00406	0.00406	0.0479	0.0479	0.0479	0.318	0.335	0.338
1.2	0.00567	0.00566	0.00564	0.0628	0.0627	0.0627	0.359	0.377	0.380
1.4	0.00711	0.00709	0.00705	0.0757	0.0756	0.0755	0.392	0.408	0.411
1.6	0.00834	0.00831	0.00830	0.0864	0.0863	0.0862	0.418	0.432	0.435
1.8	0.00935	0.00932	0.00931	0.0950	0.0949	0.0948	0.438	0.450	0.452
2.0	0.01017	0.01014	0.01013	0.1018	0.1017	0.1017	0.454	0.464	0.465
3.0	0.01228	0.01224	0.01223	0.1187	0.1189	0.1189	0.493	0.493	0.493
4.0	0.01288	0.01283	0.01282	0.1230	0.1235	0.1235	0.502	0.500	0.498
5.0	0.01306	0.01298	0.01297	0.1239	0.1247	0.1246	0.505	0.502	0.500

Two Sets of Discrete Boundary Conditions

Numerical results from three separate solutions of the example problem are compared in this section. One solution is w_N, the Navier solution that satisfies the boundary conditions

$$w = 0 \quad \frac{\partial^2 w}{\partial x^2} = 0 \qquad \text{for } x = 0 \text{ and } x = a$$

$$w = 0 \quad \frac{\partial^2 w}{\partial y^2} = 0 \qquad \text{for } y = 0 \text{ and } y = b \qquad (14)$$

at every point on the boundary.

The second solution, the extended grid solution w, is of the form of Eq. (12). The term w_E, which consists of two sets of solutions of the biharmonic equation, is a part of the solution w and contains $4(M + N)$ constants of integration, as defined in Eqs. (C3). These constants are determined by satisfying the boundary conditions for the simply supported plate [Eqs. (14)] at every node point on the plate boundary, a total of $2(M + N - 2)$ points. Two discrete boundary conditions can be written at every node point, except the four corner nodes. Each corner has three discrete conditions corresponding to the continuous conditions in Eqs. (14); $w = \partial^2 w/\partial x^2 = \partial^2 w/\partial y^2 = 0$. Therefore, only $4(M + N - 1)$ independent equations can be written for discrete boundary conditions at the node points on the plate boundary. The results reported here are computed by augmenting the equations for the discrete boundary conditions.

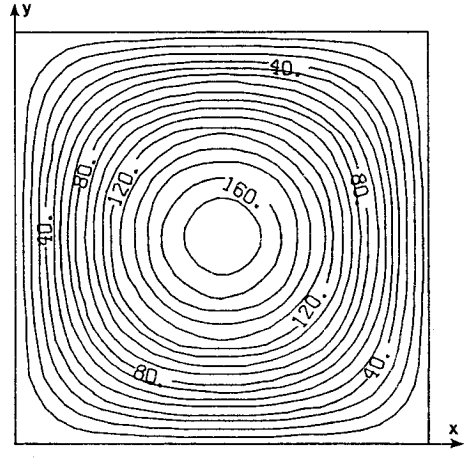

a) Discrete finite element solution

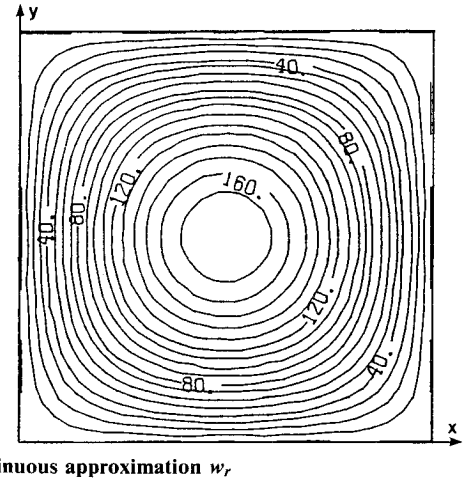

b) Continuous approximation w_r

Fig. 5 Contour plots of discrete and continuous transverse deflection w.

The augmentation consists of writing an arbitrary equation at each of the four corners of the plate. In each equation, the value of the first summation on the right-hand side of w_E in Eq. (10) is set equal to the value of the second summation. The four arbitrary relations plus the discrete boundary conditions derived from Eqs. (14) at node points on the plate boundary make a linearly independent set of equations to determine the set of $4(M + N)$ constants of integration that appear in w_E. The final result is that the extended grid solution w satifies the plate equation (2) at every node point of the $M \times N$ grid and the boundary conditions [Eqs. (14)] at every node point on the boundary.

Furthermore, since the solution is continuous and is in terms of generalized coordinates, the deflection w and stress resultants, such as bending moments and transverse shear stress resultants, can be compared to corresponding results from the Navier solution w_N at any point with coordinates (x,y) on the plate. The extended grid solution w was computed for a number of plates with different aspect ratios (a/b) and with different $M \times N$ grids. Typical results from the computations for an $M = 5$ by $N = 5$ grid and for an $M = 9$ by $N = 9$ grid are listed along with corresponding results from the Navier solution in Table 1. The number of terms in the Navier solution w_N for each result are sufficient to make those results correct for the number of digits listed in the table. As might be expected, the results based on the extended grid solution are more accurate as the number of terms increase with a finer grid. In addition, the accuracy decreases as the order of the partial derivatives increases. The moment results, which contain second partial derivatives, are more accurate than the transverse shear results, which contain third derivatives.[9]

Looking ahead to using the transformation in the extended grid in error analysis of results from general-purpose finite element codes, the third solution w_r was also computed. This solution differs from the extended grid solution w only in the details of computing the $4(M + N)$ constants of integration in w_E. The discrete boundary conditions for the w_r solution are derived from output data on rotations and deflections from a general-purpose finite element code.[1] The subscript r is used to indicate that w_r satisfies rotation boundary conditions, i.e., conditions on the partial derivative of w with respect to the

outward normal, at node points on the boundary of the plate. The four arbitrary equations at the four corners of the plate remain the same as described earlier, so that a set of $4(M + N)$ linearly independent equations is written for this more general case of matching discrete output for displacements and rotations at node points of a rectangular plate boundary. In the general case, the plate can be a skin section of a stiffened panel.[1,2]

For the example problem of the simply supported plate, matching the finite element results for rotations on the boundary allows one direct check on the finite element solution. The algorithm in that solution minimizes the potential energy subject to the geometric boundary condition on w but leaves the natural boundary conditions on the edge bending moment resultants as part of the minimization. The finite element results tabulate the bending moment resultant at centroids of the rectangular elements defined by the rectangular $M \times N$ mesh but do not estimate the residual moments on the plate boundary. The solution w_r allows direct computation of the moments at any location, including the boundary, where the moment can be large if an edge is restrained against rotation. For the simply supported case, the residual moments on the plate boundary computed from the solution w_r turn out to be small compared with the maximum moments at the center.

Plotted Results for Three Solutions

Selected results from the three solutions w_N, w, and w_r for a square plate, $a/b = 1$, are plotted in Fig. 4 along an axis of symmetry. The results show good agreement for the maximum values of the deflection w and for the moment M_x. As discussed earlier, the moment M_x from the solution w_r does not vanish at endpoints $x = 0$ and a. The small error in satisfying the boundary condition on the moment illustrates that, although the normalized residual error $E(x,y)$ is independent of the boundary conditions, the error in computing stress resultants is also a function of the error in satisfying boundary conditions. The shear stress resultant Q_x reaches its maximum value on the boundary so that its accuracy is affected both by the accuracy of the particular solution w_I and by the boundary conditions satisfied by the solution of the biharmonic equation w_E. The series for Q_x derived from the double sine series of the Navier solution w_N is slowly convergent, requiring thousands of terms to achieve three-digit accuracy. The general-purpose finite element code used to compute the moment stress resultants does not compute a direct solution for the shear stress resultants.

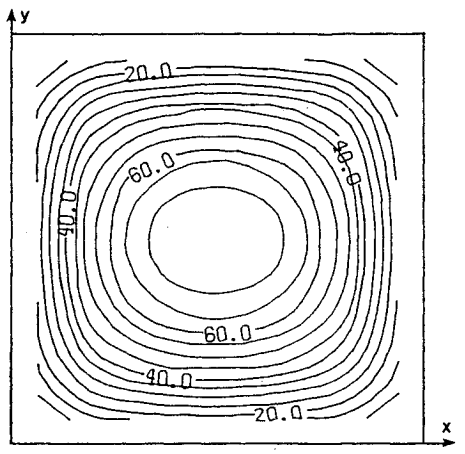

a) Discrete finite element solution

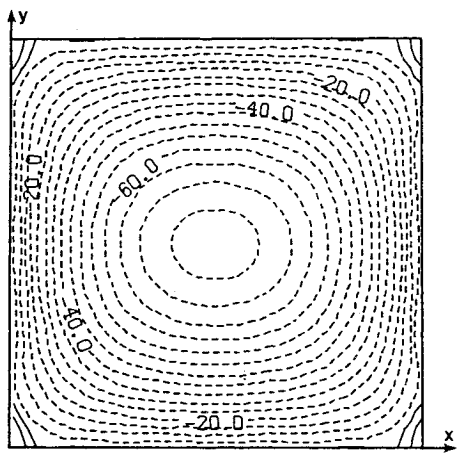

b) Continuous approximation

Fig. 6 Contour plots of discrete and continuous moment resultant M_x.

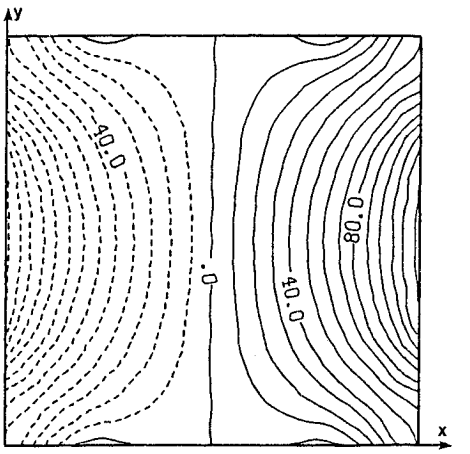

Fig. 7 Contour plots of transverse shear stress resultant Q_x.

Contour plots comparing the finite element solution and results from w_r are shown in Figs. 5–7. The results are encouraging. For example, the contour plot for the shear stress resultant Q_x shows smooth contours near the boundary. Contour plots of earlier results[1–3] for postbuckled panels are not as smooth near the boundaries, so that applying the extended grid transformation to error analysis of postbuckling results seems to be a promising approach. The numerical harmonic analysis for the slowly varying postbuckling results may converge faster than the corresponding analysis for the constant load q in Eq. (7).

Conclusions

A change of variables has been introduced in the independent variables for double Fourier sine series. When combined with numerical harmonic analysis of data tabulated on a rectangular grid, the new series passes through all of the tabulated points. When the tabulated function is nonzero on the boundary of a rectangular domain, the new series has significantly better convergence than the usual half-range Fourier series that vanishes on the boundary and exhibits Gibbs' phenomena near the boundary.

The improved convergence is illustrated by comparing the solutions of an example problem of a simply supported plate under uniform load. The example also serves to recall a general result for plate and shell problems, namely, that the error in discrete solutions for stress resultants depends on satisfying boundary conditions as well as satisfying the partial differential equations of the theory.

A solution of the biharmonic equation based on the change of variables is used to satisfy the boundary conditions for the example problem. Two series are used in this solution and satisfy boundary conditions at every boundary node point. This is compared with four series that satisfied conditions in a least-squares sense that were used in similar earlier studies of error analysis of finite element results. The numerical al-

gorithm for satisfying the boundary conditions is simpler to code for two series than for four series. The simplification will carry over when the change of variables is applied to the error analysis of finite element results for nonlinear problems.

Appendix A: One-Dimensional Series

The one-dimensional problem using the extended grid is to pass a sine series through M values of a function of x at M equally spaced values of x. The numerical analysis is slightly different than for a simple Fourier sine series. The approximation formula is intended for use in the range $0 \le x \le a$. The M discrete values of x are defined as

$$x_m = \frac{m-1}{M-1}\,a, \qquad m = 1,2,3,\ldots,M \tag{A1}$$

The approximation has the form

$$f(x) = \sum_{m=1}^{M} b_m \sin m\xi \tag{A2}$$

where

$$\xi = \frac{\pi}{M+1}\,[(x/a)(M-1)+1], \qquad 0 \le \xi \le \pi \tag{A3}$$

The coefficients b_m are determined from the summation

$$b_m = \frac{2}{M+1}\sum_{k=1}^{M} f(x_k)\sin m\xi_k \tag{A4}$$

where the sets of ξ_k are

$$\xi_k = \frac{\pi}{M+1}\,[(x_k/a)(M-1)+1]$$

$$= \frac{\pi k}{M+1} \qquad k = 1,2,3,\ldots,M \tag{A5}$$

The approximation [Eq. (A2)] will pass through the values $f(x_k)$ and through zero at $\xi = 0$ and at $\xi = \pi$, outside the range of interest for x.

The relation used to compute the Fourier coefficients b_m [Eq. (A4)] is derived from the orthogonality relation

$$\sum_{k=1}^{M} \sin i\xi_k \sin j\xi_k = \frac{M+1}{2}\,\delta_{ij} \tag{A6}$$

where δ_{ij} is the Kronecker delta,

$$\delta_{ij} = 0, \qquad \text{if } i \ne j$$

$$= 1, \qquad \text{if } i = j$$

If the sine terms in the numerical analysis are arranged to form a matrix S with elements

$$S_{ij} = \frac{\sin i\xi_j}{\sqrt{(M+1)/2}}$$

the matrix S is symmetric and orthogonal

$$S^T S = SS = I$$

In computations, it is not necessary to store the matrix or to compute each element one at a time, since all elements of the matrix are elements of a single vector V with elements

$$v_i = \sin\left\{\frac{(i-1)\pi}{M+1}\right\}, \qquad i = 1,2,3,\ldots,2M+2$$

Appendix B: Two-Dimensional Approximations

A double Fourier series to approximate a function of two variables is readily derived from the numerical analysis for a single Fourier series listed in Appendix A. The function $f(x,y)$ is known at node points of an $M \times N$ rectangular mesh. An example of such a grid is shown in Fig. 1. In the error analysis of results from finite element analysis, the nodes are corners of rectangular finite elements. The boundaries of the elements are indicated by solid lines in the figure. In the x-y coordinate system, the nodal points (x_m, y_n) are

$$x_m = \frac{m-1}{M-1}\,a, \qquad m = 1,2,3,\ldots,M \tag{B1a}$$

$$y_n = \frac{n-1}{N-1}\,b, \qquad n = 1,2,3,\ldots,N \tag{B1b}$$

The change in independent variables is indicated in the figure by the dashed lines showing the axes of the ξ-η coordinate system and (x,y) points for an extended grid of $(M+2)\times(N+2)$ points. The change in independent variables is

$$\xi = \frac{\pi}{M+1}\,[(x/a)(M-1)+1], \qquad 0 \le \xi \le \pi \tag{B2a}$$

$$\eta = \frac{\pi}{N+1}\,[(y/b)(N-1)+1], \qquad 0 \le \eta \le \pi \tag{B2b}$$

The approximation for $f(x,y)$ is written as a double-sine series,

$$f(x,y) = \sum_{m=1}^{M}\sum_{n=1}^{N} b_{mn} \sin m\xi \sin n\eta \tag{B3}$$

When the Fourier coefficients b_{mn} are computed by the formula

$$b_{mn} = \frac{4}{(M+1)(N+1)}\sum_{j=1}^{M}\sum_{k=1}^{N} f(x_j,y_k)\sin m\xi_j \sin n\eta_k \tag{B4}$$

where

$$\xi_j = \frac{\pi j}{M+1}, \qquad j = 1,2,3,\ldots,M \tag{B5a}$$

$$\eta_k = \frac{\pi k}{N+1}, \qquad k = 1,2,3,\ldots,N \tag{B5b}$$

the approximation for $f(x,y)$, is exact at the node points for the $M \times N$ grid and is zero at points on the boundary of the extended $(M+2)\times(N+2)$ grid.

In the error analysis of finite element results, the case where a function $g(x,y)$ is known at the centroids of the rectangular elements is also of interest. In that case, the centroids are the discrete points

$$\frac{x_m}{a} = \frac{2m-1}{2(M-1)}, \qquad m = 1,2,3,\ldots,M-1 \tag{B6a}$$

$$\frac{y_n}{b} = \frac{2n-1}{2(N-1)}, \qquad n = 1,2,3,\ldots,N-1 \tag{B6b}$$

The approximation for the function $g(x,y)$ is

$$g(x,y) = \sum_{m=1}^{M}\sum_{n=1}^{N} c_{mn} \sin m\xi \sin n\eta \tag{B7}$$

The Fourier coefficients are computed by the formula

$$c_{mn} = \frac{4K}{(M+1)(N+1)}\sum_{j=1}^{M-1}\sum_{k=1}^{N-1} f(x_j,y_k)\sin m\xi_j \sin n\eta_k \tag{B8}$$

where the factor K is

$$K = \frac{1}{(1 + \delta_{m\mathfrak{M}})(1 + \delta_{n\mathfrak{N}})}$$

with $\mathfrak{M} = M + 1$, $\mathfrak{N} = N + 1$, and

$$\delta_{ij} = 0, \quad \text{if } i \neq j$$
$$= 1, \quad \text{if } i = j$$

also

$$\xi_j = \frac{\pi(2j + 1)}{2(M + 1)}, \quad j = 1,2,3, \ldots, M - 1 \tag{B9a}$$

$$\eta_k = \frac{\pi(2k + 1)}{2(N + 1)}, \quad k = 1,2,3, \ldots, N - 1 \tag{B9b}$$

The approximation for $g(x,y)$ is exact at the centroids of the elements on the $M \times N$ grid, zero at centroids of the $(M + 2) \times (N + 2)$ grid that are outside the inner grid, and zero on the boundary of the extended grid.

Appendix C: Homogeneous Solutions

The functions appearing in the solution w_E in Eq. (10) that satisfy the biharmonic equation are listed in this appendix. The solution of the biharmonic equation is considered as a function of x and y. Therefore, in the expression

$$w_E = \sum_{n=1}^{N} f_n(x) \sin n\eta + \sum_{m=1}^{M} g_m(y) \sin m\xi$$

the functions of x and y are solutions of the ordinary differential equations

$$\frac{d^4 f_n}{dx^4} - 2\alpha_n^2 \frac{d^2 f_n}{dx^2} + \alpha_n^4 f_n = 0 \tag{C1a}$$

$$\frac{d^4 g_m}{dy^4} - 2\delta_m^2 \frac{d^2 g_m}{dy^2} + \delta_m^4 g_m = 0 \tag{C1b}$$

where the coefficients are defined as

$$\alpha_n = n\alpha = \frac{n\pi}{b} \frac{N - 1}{N + 1} \tag{C2a}$$

$$\delta_m = m\delta = \frac{m\pi}{a} \frac{M - 1}{M + 1} \tag{C2b}$$

The solutions are written in the form

$$f_n = A_{1n} e^{-\alpha_n x} + A_{2n} e^{-\alpha_n (a - x)} + A_{3n} \left(\frac{x}{a}\right) e^{-\alpha_n x} + A_{4n} \left(1 - \frac{x}{a}\right) e^{-\alpha_n (a - x)} \tag{C3a}$$

$$g_m = B_{1m} e^{-\delta_m y} + B_{2m} e^{-\delta_m (b - y)} + B_{3m} \left(\frac{y}{b}\right) e^{-\delta_m y} + B_{4m} \left(1 - \frac{y}{b}\right) e^{-\delta_m (b - y)} \tag{C3b}$$

where A_{kn} and B_{km} are constants of integration.

References

[1]Thurston, G. A., Reissner, J. E., Stein, P. A., and Knight, N. F., Jr., "Error Analysis and Correction of Discrete Solutions from Finite Element Codes," *AIAA Journal,* Vol. 26, No. 4, 1988, pp. 446–453.

[2]Sistla, R., and Thurston, G. A., "Error Analysis of Finite Element Solutions for Postbuckled Plates," *AIAA Journal,* Vol. 28, No. 3, 1990, pp. 515–522.

[3]Sistla, R., and Thurston, G. A., "Error Analysis of Finite Element Solutions for Postbuckled Cylinders," *Proceedings of the AIAA/ASME/ASCE/AHS 30th Structures, Structural Dynamics, and Materials Conference,* AIAA, Washington, DC, April 1989, pp. 2217–2226.

[4]Zienkiewicz, O. C., and Zhu, J. Z., "A Simple Error Estimator and Adaptive Procedure for Practical Engineering Analysis," *International Journal of Numerical Methods in Engineering,* Vol. 24, No. 2, 1987, pp. 337–357.

[5]Ainsworth, M., Zhu, J. Z., Craig, A. W., and Zienkiewicz, O. C., "Analysis of the Zienkiewicz-Zhu A-Posteriori Error Estimator in the Finite Element Method," *International Journal of Numerical Methods in Engineering,* Vol. 28, No. 9, 1989, pp. 2161–2174.

[6]Zienkiewicz, O. C., and Zhu, J. Z., "Error Estimates and Adaptive Refinements for Plate Bending Problems," *International Journal of Numerical Methods in Engineering,* Vol. 28, No. 12, 1989, pp. 2839–2853.

[7]Dow, J. O., Harwood, S., Jones, M., and Stevenson, I., "A Finite Difference Error Analysis Procedure," *Proceedings of AIAA/ASME/ASCE/AHS/ASC 31st Structures, Structural Dynamics, and Materials Conference,* AIAA, Washington, DC, 1990, pp. 1010–1022.

[8]Dow, J. O., and Byrd, D. E., "The Identification and Elimination of Artificial Stiffening Errors in Finite Elements," *International Journal of Numerical Methods in Engineering,* Vol. 26, No. 3, 1988, pp. 743–762.

[9]Timoshenko, S., and Woinowsky-Kreiger, S., *Theory of Plates and Shells,* McGraw-Hill, New York, 1959, pp. 745–747.

[10]Morse, P. M., and Feshback, H., *Methods of Theoretical Physics,* McGraw-Hill, New York, 1953, Chap. 6.

[11]Tadikonda, S. S. K., and Baruh, H., "Gibbs' Phenomenon in Structural Mechanics," *Proceedings of the AIAA/ASME/ASCE/AHS 30th Structures, Structural Dynamics, and Materials Conference,* April 1989, pp. 337–347.